IEEE Access
Multidisciplinary ⋮ Rapid Review ⋮ Open Access Journal

Received January 29, 2022, accepted February 9, 2022, date of publication February 18, 2022, date of current version March 1, 2022.

Digital Object Identifier 10.1109/ACCESS.2022.3152826

Generalized Permutation Coded OFDM-MFSK in Hybrid Powerline and Visible Light Communication

MULUNDUMINA SHIMAPONDA-NAWA[1], OLUWAFEMI KOLADE[1,2], AND LING CHENG[1], (Senior Member, IEEE)

[1]School of Electrical and Information Engineering, University of the Witwatersrand, Johannesburg, Johannesburg 2000, South Africa
[2]Department of Meteorology, University of Reading, Reading RG6 6BB, U.K.

Corresponding author: Ling Cheng (ling.cheng@wits.ac.za)

This work was supported in part by the South Africa's National Research Foundation under Grant 129311 and Grant 132651, and in part by the Mwalimu Nyerere AU Scholarship Scheme and SITA Aero.

ABSTRACT Channel impairments in powerline communication (PLC) and visible light communication (VLC) technologies are one of the causes of performance degradation in hybrid PLC and VLC (HPV) systems. In this study, we focus on one of the inherent noise types in PLC channels; impulse noise (IN), which is characterised by short bursts of rapidly modified amplitudes caused by random switching of electrical devices in a power network. Recently, a permutation coded orthogonal frequency division multiplexing (OFDM) with the M-ary frequency shift keying (MFSK) scheme, in short, PC OFDM-MFSK, was proposed for IN mitigation in PLC systems. It is conceived that the robustness of this scheme against IN in standalone PLC systems will enhance the error performance of the HPV system. Furthermore, since one of the disadvantages of the PC OFDM-MFSK scheme compared to that using only the classical OFDM scheme, is degraded data rate, we propose a generalised PC OFDM-MFSK scheme to improve the degraded data rate. This study shows that the use of OFDM-MFSK improves the performance of an HPV system compared to that using only the classical OFDM modulation scheme by a signal-to-noise (SNR) ratio gain of 6 dB at a bit error rate (BER) of 10^{-4}. Furthermore, an SNR gain of approximately 3 dB and reduction in the decoding complexity of the PC OFDM-MFSK HPV system is achieved using a soft-decision Hungarian-Murty (HM) decoder. Moreover, the generalisation of the PC OFDM-MFSK HPV system does not increase the decoding complexity when the SD HM decoder is used.

INDEX TERMS Frequency shift keying (FSK), generalized permutation coding, orthogonal frequency division multiplexing (OFDM), powerline communication (PLC), visible light communication (VLC).

I. INTRODUCTION

The hybrid communication system consisting of powerline communication (PLC) and visible light communication (VLC) technologies, is achieved based on the natural relationship between the two technologies, where the powerline is the source of electric power used by the VLC transmitters, as well as the capability of the VLC technology to transform a PLC signal into an equivalent wireless optical signal [1], [2]. As is always the case, merits and demerits of the constituent systems influence the performance of a hybrid system. Consequently, the performance of the hybrid PLC and VLC (HPV) system is negatively affected by the inherent demerits of the two constituent technologies, such as constrains by eye-safety standards, channel noise and interference. However, because of the potential that the HPV system has demonstrated, especially in terms of its application to smart cities, indoor navigation, vehicular technology, hospitals and other electromagnetic radiation restricted areas [3]–[5], continued research aimed at improving this hybrid system is inevitable.

Since its first presentation by Komine and Nakagawa [1], some research focus areas reported in literature regarding the HPV system include, PLC/VLC integration techniques

The associate editor coordinating the review of this manuscript and approving it for publication was Rui Wang.

[6]–[8], channel modelling [4], [9], modulation, multi-carrier and multi-user techniques [10]–[14], for achieving a reliable, spectral and energy efficient HPV system.

It is conceived in this work that some techniques that have been used in standalone PLC and VLC systems to mitigate their respective system demerits will enhance the performance of the HPV system. Schemes employing orthogonal frequency division multiplexing (OFDM) with M-ary frequency shift keying (MFSK) and permutation codes (PCs), have been applied to PLC systems to mitigate the impulse noise (IN) that is inherent in PLC channels [15], [16]. Therefore, we considered adapting these schemes to the HPV system investigated in this paper. Furthermore, the data rate of the HPV system using PCs, OFDM and MFSK techniques is enhanced by generalising the PC-aided system.

The use of OFDM in various communication technologies [15], [17]–[19], including HPV [11], [12], has been welcomed because it enhances spectral efficiency (SE) and is a reliable mitigation scheme against inter-symbol interference (ISI). In classical OFDM, each OFDM sub-carrier symbol carries a message symbol modulated using a single-carrier modulation technique, such as M-ary quadrature amplitude modulation (MQAM) or M-ary phase shift keying (MPSK). Furthermore, to enhance the data rate and the SE, several modulation options for OFDM-based systems such as index-based, sub-carrier number-based and shape-based OFDM schemes, have been exploited [19]–[24]. Variants of index-based OFDM include OFDM with index modulation (OFDM-IM) and spatial modulation OFDM (SM-OFDM) [20], [23], [24]. In OFDM-IM, the indices of the sub-carriers in an OFDM symbol are used to send additional information. Whereas in SM-OFDM, some information bits are mapped to and sent by the indices of antennas, while other information bits are conventionally modulated and conveyed via the activated antenna.

On the other hand, in sub-carrier number modulation OFDM (OFDM-SNM), some sub-carriers are exploited to convey additional information [21], whereas, in shape-based OFDM, the shape of pulses is exploited to convey additional information. Examples of the shaped-based OFDM modulation schemes are reported in [25], [26].

It is worth noting that the work mentioned above focused only on wireless communication systems, and some noise effects inherent in other fast varying channels such as the powerline communication (PLC), were not considered. Examples of such noise types are narrow-band (NB) noise and impulsive noise (IN), which affect multiple frequencies in the NB region [27]–[30]. In [30], where extensive measurements were carried out for a residential powerline channel, IN was observed to occur in bursts and lasting for a maximum period of about 0.1 ms. In such channels, a series of signal bits may be affected in time-domain, or a frequency may be affected during a transmit period. Therefore, special consideration in the implementation is required when index modulation (IM) of OFDM is, or its variants are applied to channels prone to NB and IN noise effects.

Since IN affects a range of frequencies in a short period [28], [30]–[33], then schemes that activate only some frequencies for data transmission at each transmit period would well mitigate this noise. This is because there is a probability that frequencies affected by the IN may not be carrying information at a particular transmit period. Hence, schemes such as MFSK where information symbols are mapped to one of the M available frequencies are good candidates for IN mitigation because only one of the M sub-carrier frequencies carries information at each sampling period.

A combination of OFDM and MFSK (OFDM-MFSK) proposed in [34]–[36], was exploited for IN mitigation in a PLC system [15]. When OFDM-MFSK, which is a variant of OFDM-IM is used, frequency sub-carriers in the OFDM symbol are segmented in groups of M, where M denotes the order of the frequency shift keying (FSK) modulation. As such, at any transmit interval, only one sub-carrier is activated in each group of M. Thus, the effects of IN are mitigated. In light of this, we extend the OFDM-MFSK scheme to an HPV system to exploit the benefits of IN mitigation, which can result in enhanced system reliability.

In [15], [16], a coded OFDM-MFSK in a PLC system was achieved with the use of PCs, whose codeword length is equal to M, the FSK modulation order. The length of a non-binary permutation codeword (PCW) is the number of integers in the codeword. In the scheme proposed in [15], a one-to-one mapping of data symbols and PCWs, was used. The non-binary PCWs' integers then determine which sub-carriers would be activated in each OFDM-MFSK sub-carrier sub-block. Each activated subcarrier conveys a set of modulated message bits and those mapped to the PCW. In this scheme, only one codeword is selected for each OFDM symbol. Therefore, all the activated sub-carriers convey the same data symbols. Therefore, if a subcarrier is affected by noise, subcarrier decoding can assist with recovering the information of the affected subcarrier. To improve the data rate of the permutation aided OFDM-MFSK scheme applied in the HPV system, we propose to select more than one codeword for each OFDM-MFSK symbol. Thus, a generalised permutation coded (GPC) OFDM-MFSK HPV system is achieved and is denoted as GPC OFDM-MFSK. Since the GPC OFDM-MFSK activates a few sub-carriers, it can be considered as a type of the recently reported sparse index modulation (SIM) [37], [38]. However, unlike SIM, where a certain number of sub-carriers are selected irrespective of the order of selection, the pattern of sub-carrier activation in GPC matters and is influenced by the positions of the integers in each selected PCW. Furthermore, since multiple PCWs are used for each OFDM symbol, the soft-decision (SD) low-complexity Hungarian-Murty (HM) decoder proposed in [39] to simultaneously detect multiple PCWs, is used.

Precisely, the contributions in this paper can be summarised as:

- To the best of our knowledge, we, for the first time, propose and present the use of the OFDM-MFSK scheme

in an HPV system to enhance the system's performance by IN mitigation.
- Increasing the OFDM-MFSK data rate by implementing a GPC scheme where k message symbols are mapped to k PCWs to be simultaneously transmitted per OFDM-MFSK symbol.
- Application of an SD HM decoder for reduced decoding complexity and further enhancement of the error rate performance of the HPV system.

The rest of the paper is organised as follows: In the following section, an overview of the OFDM-MFSK based system is presented, including the system and channel models. In Section III, the GPC OFDM-MFSK based HPV system is presented, and a brief description of the SD decoding method based on the HM decoder is also included. Then the simulation results and analysis of the different schemes considered in this work are presented in Section IV, after which the conclusion is presented in Section V.

II. OFDM-MFSK BASED HPV SYSTEM

This section first provides an overview of the basic principles of the OFDM-MFSK scheme applied to the HPV system. Later, a downlink transmission system in which the receiver is placed in a room served by a VLC transmitter installed in the ceiling, which also provides illumination, is considered. The VLC transmitter receives the information from the PLC channel and then re-transmits the information to the VLC receiver located at some position in the room of consideration.

A. AN OVERVIEW OF THE OFDM-MFSK

In M-FSK modulation, information symbols are mapped to one of the M available frequencies. Hence, one of the M frequencies is transmitted at each sampling time, resulting in $\mathcal{B}_1 = \log_2 M$ bits being transmitted at each sampling time. Thus, the bandwidth utilisation, η_1, for the MFSK scheme is given as [40],

$$\eta_1 = \frac{\mathcal{B}_1}{M}. \tag{1}$$

On the other hand, in OFDM modulation, information symbols are mapped to N orthogonal sub-carriers in an OFDM array and simultaneously transmitted in the PLC channel. If a signal constellation symbol has $\mathcal{Q}$ information bits, then $\mathcal{B}_2 = \mathcal{Q}N$ bits are transmitted per OFDM symbol. The OFDM bandwidth utilisation, η_2, can be expressed as:

$$\eta_2 = \frac{N}{N + N_{\text{cp}}}, \tag{2}$$

where N_{cp} is the number of sub-carriers used for the cyclic prefix (CP) of the OFDM symbol. A CP is inserted at the beginning of the OFDM signal to maintain orthogonality among sub-carriers. The CP consists of a cyclic extension from the end of the OFDM signal, whose length is mainly influenced by the delay spread of the channel. Thus, to eliminate ISI, inter-carrier interference (ICI) and maintain orthogonality between sub-carriers, the length of the CP is chosen to be longer than the delay spread of the channel as this ensures that all the samples from the previous OFDM symbols fall within the CP duration.

In the OFDM-MFSK scheme, N sub-carriers are divided into groups of M sub-carriers. Only one sub-carrier from each group is activated for transmission; hence, no energy is transmitted on the other $M-1$ sub-carriers in each group. Let $g = 1, 2, \ldots, G$ denote the different groups, each group consisting of M sub-carriers and $\varsigma = 1, 2, \ldots, M$ denote the indices of one of the M frequencies in a group g. Then, each of the symbols at any activated sub-carrier can be represented as $x_{g\varsigma}$. Thus, a vector representation of the whole OFDM-MFSK symbol to be transmitted per channel use via the PLC channel is

$$\boldsymbol{x} = 0 \ldots \underbrace{x_{1\varsigma}}_{\text{Group 1}} \ldots 0, 0 \ldots \underbrace{x_{2\varsigma}}_{\text{Group 2}} \ldots 0, \ldots, 0 \ldots \underbrace{x_{G\varsigma}}_{\text{Group G}} \ldots 0. \tag{3}$$

Thus, the total number of bits per OFDM-MFSK symbol is

$$\mathcal{B}_3 = G \log_2 M = G \cdot \mathcal{B}_1. \tag{4}$$

Considering (1) and (2), the bandwidth utilisation, η_3, of the OFDM-MFSK scheme can therefore be expressed as:

$$\eta_3 = \frac{\mathcal{B}_1}{M} \frac{N}{N + N_{\text{cp}}}. \tag{5}$$

Thus, the bandwidth utilisation for the MFSK, OFDM and OFDM-MFSK schemes can be compared as, $\eta_1 \leq \eta_3 < \eta_2$, indicating that the OFDM-MFSK scheme enhances the SE of the MFSK scheme, however, it is lower than that of the classical OFDM scheme.

B. SYSTEM MODEL

In Fig. 1, a system block diagram highlighting the major sections, such as the transmitter, receiver, PLC/VLC integration module and the channels, of the OFDM-MFSK HPV system, is shown.

1) PLC SECTION AND THE INTEGRATION UNIT

The incoming modulated symbols are segmented into $G = \frac{N}{M}$ groups, and each information symbol in a particular group determines the sub-carrier index to be activated for transmission. The frequency-domain signals are converted to the time-domain via the inverse fast Fourier transform (IFFT) block and transmitted via the PLC channel. At the PLC/VLC integration module, the output signal from the PLC channel is given by

$$\boldsymbol{y}_{\text{p}} = \boldsymbol{s} \cdot e^{j\phi} + \boldsymbol{n}_{PLC}. \tag{6}$$

In (6), $\boldsymbol{s}$ is the complex transmitted signal and $\boldsymbol{n}_{PLC} = \boldsymbol{n}_G + \boldsymbol{n}_I\sqrt{z}$, is the noise component in the PLC channel comprising the background noise and the IN denoted as $\boldsymbol{n}_G$ and $\boldsymbol{n}_I$, respectively. $\boldsymbol{n}_G$ is modelled as an additive white Gaussian noise (AWGN) (a complex component with zero-mean and variance of $\sigma_G^2 = 2N_0$, where N_0 denotes noise power spectral

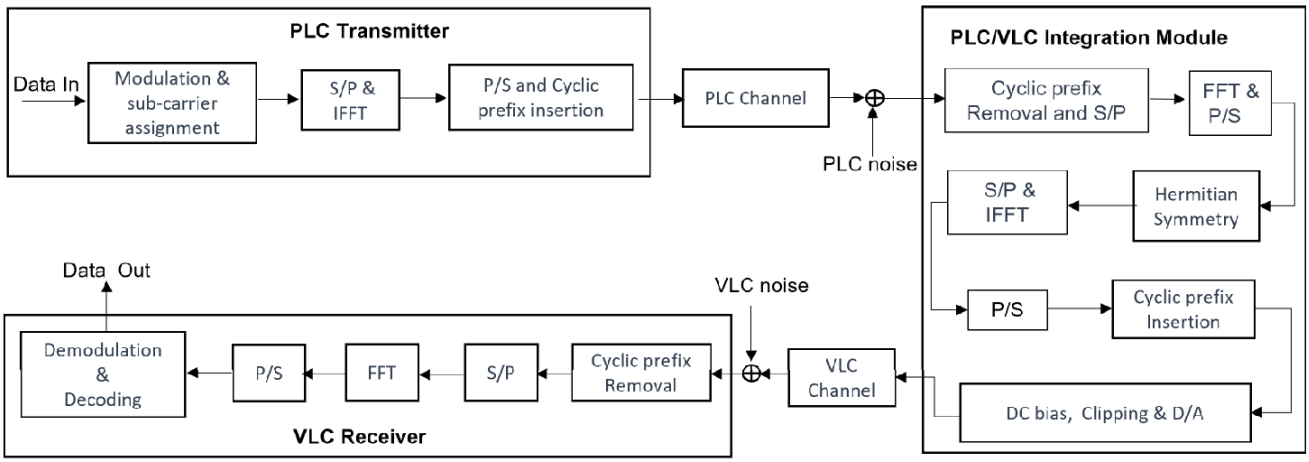

FIGURE 1. System block diagram of the OFDM-*M*FSK HPV system.

density) and $\boldsymbol{n}_I$ follows a Poisson distribution and has a variance σ_G^2/A. A is the impulsive index that determines the frequency of occurrence of $\boldsymbol{n}_I$ and z is a variable imposing the Poisson distribution on $\boldsymbol{n}_I$. If the amplify-and-forward (AF) relaying protocol is applied, the received PLC signal $\boldsymbol{y}_\mathrm{p}$ is demodulated, scaled, and re-modulated [12]. The resulting signal is re-transmitted by VLC transmitters. On the other hand, the decode-and-forward (DF) relaying protocol will also decode the received PLC signal before re-modulation for transmission by the VLC transmitters. In this work, the AF relaying protocol is assumed for its simplicity.

2) VLC SECTION

The signal $\boldsymbol{y}_\mathrm{p}$ at the fast Fourier transform (FFT) output, in the integration unit, is complex. Since the VLC section of the HPV system employs intensity-modulation direct-detection (IM/DD), $\boldsymbol{y}_\mathrm{p}$ is unsuitable for modulating the intensity of the VLC transmitters due to the constraint that light intensity cannot be negative. To obtain optical IM/DD compatible signals, the Hermitian symmetry (HS) property to generate real OFDM signals has widely been used [10], [12], [41]. In an HS structure, a message symbol is duplicated in the form of its complex conjugate (CC). For the N frequency-domain symbols obtained from the FFT operation on PLC output signal, the general expression relating the message symbols X, their CC X^* components and their positions due to the HS constraint is given as:

$$X_{(\xi+2)} = X^*_{(2N-\xi)}, \quad \xi = 0, 1, 2, \ldots, N-2. \tag{7}$$

Thus, the HS structure is formed by concatenating the original vector of message symbols with the vector of their CC symbols. From (7), it can be seen that in VLC, $2N$ sub-carriers are required due to the HS constraint. If the same number of sub-carriers is maintained between the PLC and VLC channels, then the symbols from the PLC would be transmitted in two transmit periods. Another way would be to apply the HS constraint at the PLC section. Then, the same number of sub-carriers would be maintained between the two channels. In the HS structure, the first and $(N+1)^{th}$ components are set to zero to avoid any DC shift or any residual complex component in the time-domain signal, $(X_{(0)} = X_{(N+1)} = 0)$.

After the HS block, the signal is again converted to a time-domain signal $\boldsymbol{x}_\mathrm{v}$ by the IFFT. Then, a CP is inserted at the beginning of the OFDM signal to maintain orthogonality among sub-carriers. The signal $\boldsymbol{x}_\mathrm{v}$ is real-valued and bipolar with a random-like variation often characterized by a high peak-to-average power ratio (PAPR) [12], [42]. The high PAPR leads to signal distortions due to the non-negativity constraint for the optical time-domain signal and a reduced energy efficiency for practical LED drivers with limited dynamic ranges [12]. As such, a DC bias is then added to $\boldsymbol{x}_\mathrm{v}$ in order to make the signal compatible with IM/DD channel and avoid the PAPR problem. Additionally, before modulating the LED, peaks of time-domain OFDM signals may be clipped at the voltage, which corresponds to permissible pulsed currents recommended by the manufacturer [42]. However, this may introduce clipping noise, as will be shown in Section IV. After the digital-to-analogue (D/A) operation, $\boldsymbol{x}_\mathrm{v}$ modulates the LEDs transmitters for transmission via the VLC wireless channel. The transmitters are assumed to have a Lambertian propagation model.

In this paper, only the LOS component is assumed as it accounts for a greater portion of the transmitted optical signal [18], [43]. The channel gain, considering an LOS propagation between a transmitter and a receiver located at a distance of d_v and angle of irradiance θ, with respect to the transmitter, can be approximated as [44],

$$h = \begin{cases} \dfrac{A_r(\ell+1)}{2\pi d^2} cos^{\ell}(\theta) cos(\psi), & 0 \le \psi \le \Psi_c \\ 0, & \text{elsewhere,} \end{cases} \tag{8}$$

where A_r is the effective collection area of the detector, ψ is the angle of incidence with respect to the receiver axis and ℓ is the Lambertian emission order given by $\ell = -\frac{\text{-ln2}}{\ln cos(\Phi_{1/2})}$.

$\Phi_{1/2}$ is the semi-angle at half power of the transmitter. The received optical signal at any receiver element is expressed as:

$$\boldsymbol{y}_{\mathrm{v}} = \boldsymbol{x}_{\mathrm{v}} \cdot h + \boldsymbol{n}_{G\mathrm{v}}, \tag{9}$$

where $\boldsymbol{n}_{G\mathrm{v}}$ denotes the noise which is modeled as AWGN with zero-mean (as used in (6)) and variance $\sigma^2_{G\mathrm{v}}$. In the VLC receiver, the CP is first removed and the signal is passed through a serial-to-parallel (S/P) converter before the FFT is performed on the signal.

The estimation of the likely transmitted symbols can be achieved by maximum likelihood (ML) detection. In [45] envelope detection was used for estimating MFSK in AWGN, while the analysis in [34] suggests that the decision for estimating the transmitted signal is made in favour of the maximum absolute value of the components of $\boldsymbol{y}_{\mathrm{v}}$. As these are similar, the analysis and expression in [34] is adopted, and the vector $\hat{\boldsymbol{y}}_{\mathrm{v}}$ consisting of the estimated transmitted symbols is given as:

$$\hat{\boldsymbol{y}}_{\mathrm{v}} = \underset{\boldsymbol{x}_{\mathrm{v}} \in F}{\arg\max} \, |\boldsymbol{y}_{\mathrm{v}} \boldsymbol{x}_{\mathrm{v}}|^2. \tag{10}$$

Note that $\boldsymbol{x}_{\mathrm{v}}$ is a vector consisting of different $x_{\mathrm{v}_{g\varsigma}}$ elements from one of the activated sub-carriers in the OFDM array F, where variables g and ς denote the group and sub-carrier index in that group.

The bit error probability, P_e of OFDM-MFSK, for the energy per bit, E_b, is said to be the same as that of the MFSK [15] and is defined as:

$$P(e) = \sum_{\varsigma=1}^{M-1} \frac{(-1)^{\varsigma+1}}{\varsigma+1} \binom{M-1}{\varsigma} e^{\left(-\frac{\varsigma \log_2 M}{M+1} \frac{E_b}{N_0}\right)}. \tag{11}$$

Larger M values would enhance the error performance of the system, however, this degrades the SE. Hence, a trade-off between error performance and SE is inevitable.

III. GENERALISED PERMUTATION-CODED OFDM-MFSK HPV SYSTEM

In this section, we present a method to improve the data rate of the OFDM-MFSK HPV system by employing PCs. Precisely, the use of PCs is also considered to aid the use of a soft-decision method of identifying the activated sub-carriers of the OFDM-MFSK scheme. First, the model of a permutation-coded OFDM-MFSK (PC OFDM-MFSK) system is presented and then the generalised scheme is presented.

A. PERMUTATION CODED OFDM-MFSK HPV SYSTEM

In this section, the idea of sub-carrier coding of the OFDM-MFSK [15], [16] was extended to the HPV system introduced in Section II. A permutation codebook $\boldsymbol{P}$ consists of $|\boldsymbol{P}|$ codewords of length M [46]. All $|\boldsymbol{P}|$ codewords in $\boldsymbol{P}$ are row vectors denoted in this work by $\boldsymbol{v}_p$ and contain M different integers $1, 2, \ldots, M$, as symbols, while $p = 1, 2, \ldots, |\boldsymbol{P}|$. Hence,

$$b_1 = \lfloor \log_2 |\boldsymbol{P}| \rfloor, \tag{12}$$

bits are mapped per each codeword $\boldsymbol{v}_p$, where $\lfloor . \rfloor$ denotes the floor function. Each $\boldsymbol{v}_p \in \boldsymbol{P}$ can be converted to an equivalent $[0, 1]^{M \times M}$ codeword matrix $\boldsymbol{C}_p = [c_{ij}]$ such that in each column of $\boldsymbol{C}_p$, a '1' fills the position which corresponds to the integer of the codeword, while other $M - 1$ values in the column are set to '0'.

1) SYSTEM MODEL FOR THE PERMUTATION-CODED OFDM-MFSK HPV SYSTEM

In PC OFDM-MFSK, b_1 information bits are mapped to a predefined PCW, $\boldsymbol{v}_p$. Note that in this work, the length of PCWs and the MFSK order are assumed equal; they both have the same value of M. Therefore, even in PC OFDM-MFSK, G groups of sub-carriers are formed by $\frac{N}{M}$ and each integer symbol in $\boldsymbol{v}_p$ indicates the index of the active sub-carrier in each of the G groups. The sequence of b_1 bits is repeated over each active sub-carrier. Therefore, in addition to the information bits mapped to modulation constellation symbols, the PC OFDM-MFSK data rate is enhanced by b_1 bits mapped to each index of the activated sub-carrier. As such, the total number of transmitted bits $\mathcal{B}_4$ in a PC OFDM-MFSK, per channel use is,

$$\mathcal{B}_4 = b_1 + \mathcal{B}_3 = b_1 + G \cdot \mathcal{B}_1. \tag{13}$$

2) SOFT-DECISION DECODING FOR PC OFDM-MFSK HPV SYSTEM

Suppose the transmitted information symbols are mapped to conventional modulation constellations and the index of the PCW. In that case, the receiver's task is to estimate the digitally modulated information symbols and those mapped to the PCWs. The digitally modulated symbols are conventionally demodulated and estimated according to the appropriate scheme matching the modulation technique used at the transmitter. At the same time, those mapped to PCWs are recovered after detecting the corresponding codewords. An iterative SD decoder based on the Hungarian and Murty's algorithms described in [39], is employed to enhance decoding reliability as well as reduce the decoding complexity of the PC OFDM-MFSK HPV system.

The SD decoders in [16], [39], [47] consider the signal input, $\boldsymbol{Y}_{\mathrm{v}} = [(y_{\mathrm{v}})_{ij}] \in \mathcal{C}^{M \times M}$, as an assignment problem, such that a linear programming algorithm based on the Hungarian method [48], is employed for decoding. The mathematical model of an assignment problem [48], can be expressed as:

$$K = \sum_{i=1}^{M} \sum_{j=1}^{M} c_{ij} (y_{\mathrm{v}})_{ij}, \tag{14}$$

subject to the constraints

$$\sum_{i=1}^{M} c_{ij} = \sum_{j=1}^{M} c_{ij} = 1, \quad (i, j = 1, 2, \ldots, M), \tag{15}$$

where K in (14) is the cost of the assignment and $(y_{\mathrm{v}})_{ij}$ is the cost of assigning a resource to an activity.

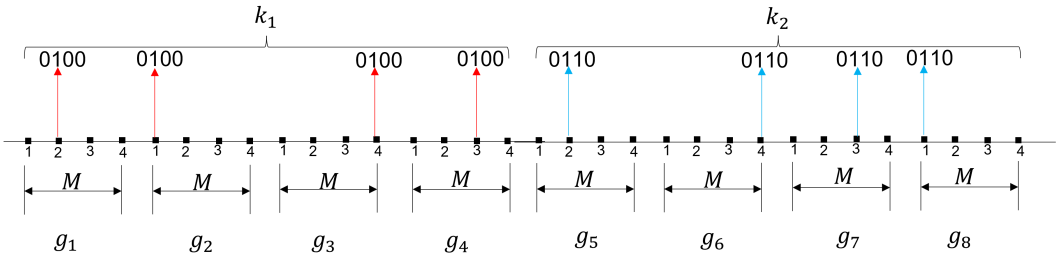

FIGURE 2. Representation of encoded bits mapped to PCs in a GPC OFDM-MFSK. $N = 32$, $k = 2$, $M = 4$. The encoded bits 0100 and 0110 are mapped to 2143 and 2431, respectively.

From the model in (14), the Hungarian algorithm of the HM decoder iteratively finds an $M \times M$ matrix $\boldsymbol{R} = [r_{ij}] \in \mathbb{R}$ that produces the maximum cost K corresponding to $\boldsymbol{v}_p$. If the produced codeword $\boldsymbol{v}_p \in \boldsymbol{P}$, then the decoder stops and the produced codeword is assumed to be the transmitted codeword. However, suppose the produced codeword does not belong to $\boldsymbol{P}$, then from $\boldsymbol{R}$, using Murty's algorithm, the decoder finds the next highest $\mathcal{K}$ costs and ranks them in order of decreasing cost. The highest-ranking cost corresponding to one of $\boldsymbol{v}_p \in \boldsymbol{P}$, is then selected to be the transmitted codeword. Let $\boldsymbol{y}_{\mathrm{v}} = vec(\boldsymbol{Y}_{\mathrm{v}})$ denote the HM decoder input. The HM decoding algorithm can be summarised and presented as follows:

Algorithm 1 HM Decoding in PC OFDM-MFSK HPV System

Input: Channel output matrix $\boldsymbol{Y}_{\mathbf{v}} = [(y_{\mathrm{v}})_{ij}] \in \mathcal{C}^{M\times M}$ in
Output: PCW $\boldsymbol{v}_p$ out

1: By Hungarian method, find matrix $\boldsymbol{R} = [r_{ij}] \in \mathbb{R}$
2: **if** $\boldsymbol{v}_p \in \boldsymbol{P}$ **then**
3: $\boldsymbol{v}_p$ is the transmitted PCW
4: Stop decoder process
{Complexity order of $O(M^3)$ [49]}
5: **else**
6: By Murty's algorithm, find the best $\mathcal{K}$ PCWs and rank them in order of increasing cost.
7: Select $\boldsymbol{v}_p$ corresponding to the highest-ranking cost as the transmitted codeword
{Complexity order of $O(M^4)$ [50]}
8: **end if**
{The overall worst-case decoder complexity order is $O(M^4)$}

B. GENERALISATION OF THE PC OFDM-MFSK BASED HPV SYSTEM

In generalising the PC OFDM-MFSK scheme, N sub-carriers are divided into $G = \frac{N}{M}$ groups of M sub-carriers each, similar to the PC OFDM-MFSK scheme. However, the G groups are further divided into $k = \frac{G}{M}$, as illustrated in Fig. 2. Each k group is mapped to a sequence of b_1 bits. As such, a set of $k > 1$ codeword indices are transmitted at a time.

Consequently, the number of bits mapped to PCWs is improved by a factor of k. Hence,

$$b_2 = k\lfloor \log_2 |\boldsymbol{P}| \rfloor = k \cdot b_1. \tag{16}$$

Therefore, the total number of transmitted bits $\mathcal{B}_5$ in a GPC OFDM-MFSK, per channel use is,

$$\mathcal{B}_5 = b_2 + \mathcal{B}_3 = k \cdot b_1 + G \cdot \mathcal{B}_1. \tag{17}$$

When decoding by hard-decision (HD), minimum distance decoding is used, where the sequence of the received vector is compared to all possible combination sequences. However, this method exponentially increases in complexity with the increase in code length M and k. In this work, because multiple codewords are transmitted for each OFDM-MFSK symbol, we elect to use the SD HM decoder applied in a multiple access system in [39]. At the receiver, elements from each k group are represented as $M \times M$ matrices, after which all the matrices are added together to form the decoder input, $\boldsymbol{Y}_{\mathrm{v}} = [(y_{\mathrm{v}})_{ij}]$. Then, the HM decoding algorithm is applied as in the case of the PC OFDM-MFSK system. However, unlike the decoding in Section III-A2, where the decoder can stop at the Hungarian stage, when the HM decoder is applied to the GPC-OFDM-MFSK, Murty's algorithm is mandatory. The decoder must select the k highest costs corresponding to the k codewords mapped to the transmitted message symbols. Nevertheless, the decoding complexity in the GPC system is still $O(M^4)$.

IV. SIMULATION AND RESULTS ANALYSIS

A series of performance simulations for the classical OFDM, OFDM-MFSK, PC OFDM-MFSK and GPC-OFDM-MFSK systems, are carried out and their results compared. A VLC transmitter controlled and receiving information from the powerline is installed at a height of 3 m above the floor. The transmitter has a half-power angle of $(\Phi_{1/2}) = 15°$. The receiver placed at 0.85 m above the floor is a photo-detector with an angle of incidence $\psi = 70°$ while $A_r = 1 \times 10^{-4}$ m. For all coded systems, we apply a permutation codebook defined by $\mathcal{PC}(M = 4, d_{\min} = 3)$.

A. BER PERFORMANCE COMPARISON OF OFDM HPV AND OFDM-MFSK HPV SYSTEMS

In Fig. 3, the BER performance of the OFDM-MFSK HPV system is presented and compared to that of the classical

OFDM HPV system. The simulation was carried out for $N = 32$ and 512, using two simple DC biasing methods referred to as DC1 and DC2. In the DC1 biasing method, the DC bias added to all the components at the output of the IFFT block is equal to the minimum absolute value of the real bipolar signal at the output of the IFFT block, DC1 $= \min(|\boldsymbol{x}_v|)$. On the other hand, DC2 biasing refers to a bias of $10\log_{10}(\zeta^2 + 1)$ [51], where ζ, is the clipping factor. The robustness against IN due to MFSK in the OFDM-MFSK based HPV system is evident as all the performance graphs show its superior performance over that of the classical OFDM-based HPV system. For instance, at a BER of 10^{-3}, over 5 dB and 3 dB differences are recorded for the DC1 graphs using $N = 32$ and 512, respectively. A trade-off between higher data rates and system reliability is inevitable, evidenced by the better performance obtained when smaller values of N are used for signal-to-noise ratio (SNR) values below 20 dB. The performance difference at 10^{-3} between the OFDM-MFSK systems of $N = 32$ to that of $N = 512$ is over 1 dB. However, at higher SNR, systems with larger values of N show better reliability, especially for the classical system.

B. DC BIASING AND CLIPPING EFFECTS ON BER PERFORMANCE OF THE OFDM HPV AND OFDM-MFSK HPV SYSTEMS

The impact of the two DC biasing methods mentioned in Section IV-A and clipping on the BER performance are analysed. In Fig. 3, the DC1 method achieves better results than the DC2 method. This could be attributed to the fact that when DC2 is used, there are some signal components with negative picks that are clipped to zero, resulting in information loss. For OFDM-MFSK, which only activates a subset of sub-carriers, the ratio of information loss would be higher. In light of the performance results of the two DC biasing methods, the subsequent simulations are based on the DC1 method since it achieves better results.

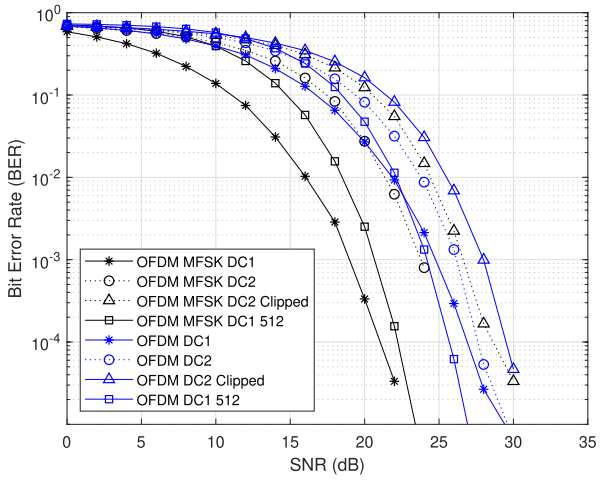

FIGURE 3. BER performance comparison of OFDM and OFDM-MFSK for varying sub-carrier window sizes, N.

C. CODED AND UNCODED OFDM-MFSK BASED HPV SYSTEM

Fig. 4 shows the BER performance of the permutation coded and uncoded systems, labelled as PC OFDM-MFSK and OFDM-MFSK, respectively. Both systems use the HD decoder. The performance of the two systems are comparable, which can be attributed to the fact that both systems allow the activation of only one sub-carrier in each group of M; hence the effect on the IN mitigation is similar.

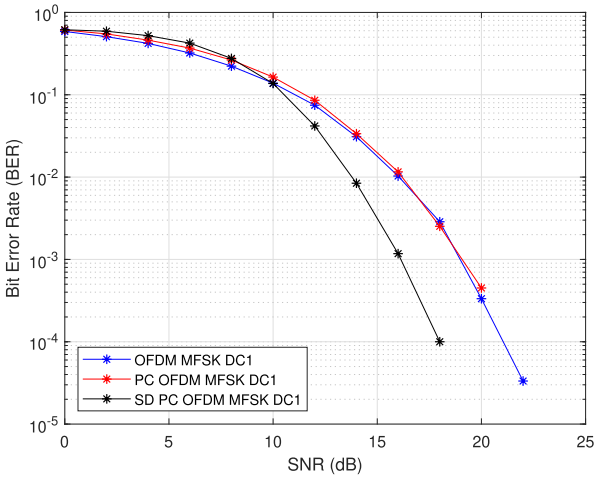

FIGURE 4. Hard-decision versus soft-decision decoding. $A = 0.1$.

Furthermore, an SD decoder was employed, and its performance compared to that of the HD based decoders. Because of the Hungarian-based SD decoder's iterative feature, its reliability is enhanced compared to that using the HD decoder. Additionally, as presented in [39], the complexity of the HD decoder is exponential with respect to the length of the permutation code, while that of the SD decoder based on the Hungarian and Murty's algorithms is polynomial. Hence, using the SD decoder enhances the system reliability and offers a lower decoding complexity.

D. IMPULSE NOISE EFFECTS

In Fig. 5, the system reliability of the investigated schemes for different values of the parameter A, is presented. The results in Fig. 5 can be seen to depict the system reliability at different times of the day for indoor environments. Values of $A = 0.01$ and 0.1 were simulated. At lower SNR values, systems simulated with $A = 0.01$ show a lower error probability. However, as the SNR increases, the independence on A in multi-carrier modulations mentioned in [28] is evident, where the performance of the systems modelled with $A = 0.1$ show an improvement.

E. GPC OFDM-MFSK HPV SYSTEM PERFORMANCE

1) BIT ERROR RATE PERFORMANCE

The performance of the GPC OFDM-MFSK based HPV system is illustrated in Fig. 5. The bit error rate (BER) performance is simulated only for information symbols mapped

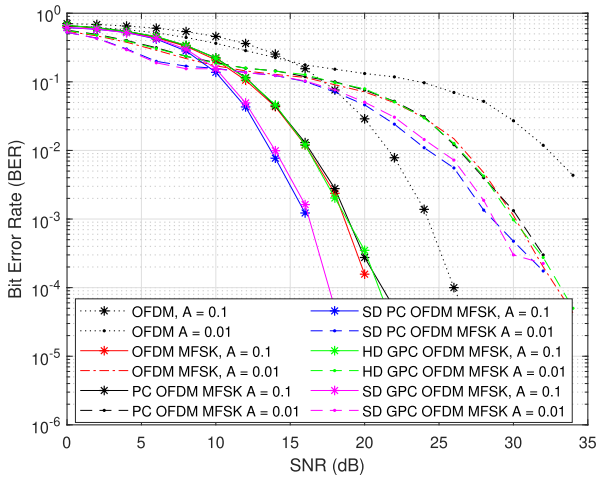

FIGURE 5. Effect of varying *A* values on BER performance for the OFDM, coded and uncoded OFDM-*M*FSK based HPV systems, including the GPC based system.

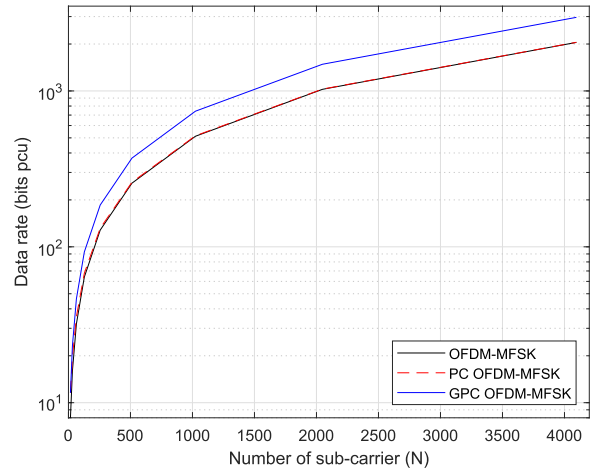

FIGURE 6. Data rate comparison for OFDM-*M*FSK, PC OFDM-*M*FSK and GPC OFDM-*M*FSK scheme for $\mathcal{PC}(M = 4, d_{\min} = 3)$ with varying *N*.

to the PCWs, without including those from a modulation constellation. We notice that the GPC graphs simulated with $A = 0.1$ and 0.01 for both HD and SD decoders almost match those of the PC OFDM-*M*FSK based systems. This could be attributed to the fact that there is no increase in the number of sub-carriers activated in each group of M. Hence, the IN mitigation feature of *M*FSK is preserved with an increased system data rate.

2) DATA RATE COMPARISON

A data rate comparison for OFDM-*M*FSK, PC OFDM-*M*FSK and GPC OFDM-*M*FSK schemes, for $\mathcal{PC}(M = 4, d_{\min} = 3)$ and varying N, is shown in Fig. 6. Due to the fact that bits mapped to PCWs are repeated for all activated sub-carriers, the data rate enhancement of the PC OFDM-*M*FSK scheme does not show a significant difference over the OFDM-*M*FSK scheme. However, it is noticed that with increasing N values for the same M, generalising the PC OFDM-*M*FSK scheme enhances the system data rate. For instance, for $N = 2048$, the data rate ratio increase for $\mathcal{B}_5$ to $\mathcal{B}_4$, is approximately 0.4. Thus, with the BER performance matching that of the PC OFDM-*M*FSK as shown in Fig. 5, using the GPC OFDM-*M*FSK scheme for the HPV system would enhance both the reliability and data rate.

V. CONCLUSION

The use of OFDM-*M*FSK enhances the BER performance of the HPV communication system. In the OFDM-*M*FSK, only a selected set of sub-carriers are activated to transmit information bits for each OFDM symbol; hence the ratio of sub-carriers that can be affected in each g group is reduced to $\frac{1}{M}$. The robustness of the OFDM-*M*FSK scheme against IN enhances the system reliability compared to that using the classical OFDM scheme. An SNR gain of 5 dB was achieved at a BER of 10^{-3}. Further, in order to use the soft-decision low-complexity decoder based on the Hungarian and Murty's algorithms, PCs were used to determine the sub-carriers to be activated for each transmitted OFDM symbol. In addition, the issue of the reduced data rate in the HPV system employing the OFDM-*M*FSK scheme is addressed by implementing a GPC scheme. In the GPC scheme, the data rate is enhanced by a factor k, which denotes the number of PCWs that can simultaneously be transmitted per OFDM-*M*FSK symbol and can uniquely be decoded. Since the GPC scheme also activates only one sub-carrier per group of M as in the PC OFDM-*M*FSK scheme, the OFDM-*M*FSK feature is maintained; hence IN is still well mitigated. Moreover, the system decoding complexity is maintained when the HM SD decoder is used. To further enhance the performance of the GPC OFDM-*M*FSK scheme, other potentially less complex detection methods based on the sparse nature of the activated sub-carriers, can be considered for future work.

REFERENCES

[1] T. Komine and M. Nakagawa, "Integrated system of white LED visible-light communication and power-line communication," *IEEE Trans. Consum. Electron.*, vol. 49, no. 1, pp. 71–79, Feb. 2003.

[2] S. M. Nlom, A. R. Ndjiongue, and K. Ouahada, "Cascaded PLC-VLC channel: An indoor measurements campaign," *IEEE Access*, vol. 6, pp. 25230–25239, 2018.

[3] W. Ding, F. Yang, H. Yang, J. Wang, X. Wang, X. Zhang, and J. Song, "A hybrid power line and visible light communication system for indoor hospital applications," *Comput. Ind.*, vol. 68, pp. 170–178, Apr. 2015.

[4] O. Kolade and L. Cheng, "Memory channel models of a hybrid PLC-VLC link for a smart underground mine," *IEEE Internet Things J.*, early access, Dec. 2, 2021, doi: 10.1109/JIOT.2021.3132129.

[5] W.-W. Hu, F.-L. Chang, Y.-H. Zhang, L.-B. Chen, C.-T. Yu, and W.-J. Chang, "Design and implementation of a next-generation hybrid Internet of Vehicles communication system for driving safety," *J. Commun.*, vol. 13, no. 12, pp. 737–742, Dec. 2018.

[6] H. Ma, L. Lampe, and S. Hranilovic, "Integration of indoor visible light and power line communication systems," in *Proc. IEEE 17th Int. Symp. Power Line Commun. Its Appl.*, Mar. 2013, pp. 291–296.

[7] M. S. A. Mossaad, S. Hranilovic, and L. Lampe, "Amplify-and-forward integration of power line and visible light communications," in *Proc. IEEE Global Conf. Signal Inf. Process. (GlobalSIP)*, Dec. 2015, pp. 1322–1326.

[8] O. Kolade, A. D. Familua, and L. Cheng, "Indoor amplify-and-forward power-line and visible light communication channel model based on a semi-hidden Markov model," *AEU Int. J. Electron. Commun.*, vol. 124, Sep. 2020, Art. no. 153108.

[9] A. D. Familua, A. R. Ndjiongue, K. Ogunyanda, L. Cheng, H. C. Ferreira, and T. G. Swart, "A semi-hidden Markov modeling of a low complexity FSK-OOK in-house PLC and VLC integration," in *Proc. IEEE Int. Symp. Power Line Commun. Appl. (ISPLC)*, Mar. 2015, pp. 199–204.

[10] X. Ma, J. Gao, F. Yang, W. Ding, H. Yang, and J. Song, "Integrated power line and visible light communication system compatible with multi-service transmission," *IET Commun.*, vol. 11, no. 1, pp. 104–111, 2017.

[11] T. Komine, S. Haruyama, and M. Nakagawa, "Performance evaluation of narrowband OFDM on integrated system of power line communication and visible light wireless communication," in *Proc. 1st Int. Symp. Wireless Pervasive Comput.*, Jan. 2006, p. 6 pp.–6.

[12] H. Ma, L. Lampe, and S. Hranilovic, "Hybrid visible light and power line communication for indoor multiuser downlink," *IEEE/OSA J. Opt. Commun. Netw.*, vol. 9, no. 8, pp. 635–647, Aug. 2017.

[13] J. Gao, F. Yang, and W. Ding, "Novel integrated power line and visible light communication system with bit division multiplexing," in *Proc. Int. Wireless Commun. Mobile Comput. Conf. (IWCMC)*, Aug. 2015, pp. 680–684.

[14] S. Feng, T. Bai, and L. Hanzo, "Joint power allocation for the multi-user NOMA-downlink in a power-line-fed VLC network," *IEEE Trans. Veh. Technol.*, vol. 68, no. 5, pp. 5185–5190, May 2019.

[15] O. Kolade and L. Cheng, "Impulse noise mitigation using subcarrier coding of OFDM-MFSK scheme in powerline channel," in *Proc. IEEE Int. Conf. Commun., Control, Comput. Technol. for Smart Grids (SmartGridComm)*, Oct. 2019, pp. 1–6.

[16] O. Kolade, A. M. Abu-Mahfouz, and L. Cheng, "A subcarrier permutation scheme for noise mitigation and multi-access in powerline channels," in *Proc. IEEE Int. Symp. Power Line Commun. its Appl. (ISPLC)*, Oct. 2021, pp. 19–24.

[17] Y. Sun, F. Yang, and L. Cheng, "An overview of OFDM-based visible light communication systems from the perspective of energy efficiency versus spectral efficiency," *IEEE Access*, vol. 6, pp. 60824–60833, 2018.

[18] M. S. A. Mossaad, S. Hranilovic, and L. Lampe, "Visible light communications using OFDM and multiple LEDs," *IEEE Trans. Commun.*, vol. 63, no. 11, pp. 4304–4313, Nov. 2015.

[19] A. M. Jaradat, J. M. Hamamreh, and H. Arslan, "Modulation options for OFDM-based waveforms: Classification, comparison, and future directions," *IEEE Access*, vol. 7, pp. 17263–17278, 2019.

[20] E. Başar, U. Aygölü, E. Panayırcı, and H. V. Poor, "Orthogonal frequency division multiplexing with index modulation," *IEEE Trans. Signal Process.*, vol. 61, no. 22, pp. 5536–5549, Nov. 2013.

[21] A. M. Jaradat, J. M. Hamamreh, and H. Arslan, "OFDM with subcarrier number modulation," *IEEE Wireless Commun. Lett.*, vol. 7, no. 6, pp. 914–917, Dec. 2018.

[22] R. Fan, Y. J. Yu, and Y. L. Guan, "Generalization of orthogonal frequency division multiplexing with index modulation," *IEEE Trans. Wireless Commun.*, vol. 14, no. 10, pp. 5350–5359, Oct. 2015.

[23] S. Ganesan, R. Mesleh, H. Ho, C. W. Ahn, and S. Yun, "On the performance of spatial modulation OFDM," in *Proc. Fortieth Asilomar Conf. Signals, Syst. Comput.*, Oct. 2006, pp. 1825–1829.

[24] E. Başar, "Index modulation techniques for 5G wireless networks," *IEEE Commun. Mag.*, vol. 54, no. 7, pp. 168–175, Jul. 2016.

[25] G. Fettweis, M. Krondorf, and S. Bittner, "GFDM–Generalized frequency division multiplexing," in *Proc. IEEE 69th Veh. Technol. Conf. (VTC Spring)*, Apr. 2009, pp. 1–4.

[26] E. Catak and L. Durak-Ata, "An efficient transceiver design for superimposed waveforms with orthogonal polynomials," in *Proc. IEEE Int. Black Sea Conf. Commun. Netw. (BlackSeaCom)*, Jun. 2017, pp. 1–5.

[27] D. Middleton, "Statistical-physical models of electromagnetic interference," *IEEE Trans. Electromagn. Compat.*, vol. EMC–19, no. 3, pp. 106–127, Aug. 1977.

[28] T. Shongwe, A. J. H. Vinck, and H. C. Ferreira, "A study on impulse noise and its models," *SAIEE Afr. Res. J.*, vol. 106, no. 3, pp. 119–131, Sep. 2015.

[29] A. Mengi and A. J. H. Vinck, "Successive impulsive noise suppression in OFDM," in *Proc. ISPLC*, 2010, pp. 33–37.

[30] O. G. Hooijen, "On the channel capacity of the residential power circuit used as a digital communications medium," *IEEE Commun. Lett.*, vol. 2, no. 10, pp. 267–268, Oct. 1998.

[31] N. Andreadou and F. N. Pavlidou, "PLC channel: Impulsive noise modelling and its performance evaluation under different array coding schemes," *IEEE Trans. Power Del.*, vol. 24, no. 2, pp. 585–595, Apr. 2009.

[32] L. Di Bert, P. Caldera, D. Schwingshackl, and A. M. Tonello, "On noise modeling for power line communications," in *Proc. IEEE Int. Symp. Power Line Commun. Appl.*, Apr. 2011, pp. 283–288.

[33] G. Al-Juboori, E. Tsimbalo, A. Doufexi, and A. R. Nix, "A comparison of OFDM and GFDM-based MFSK modulation schemes for robust IoT applications," in *Proc. IEEE 85th Veh. Technol. Conf. (VTC Spring)*, Jun. 2017, pp. 1–5.

[34] E. Peiker-Feil, M. Wetz, W. G. Teich, and J. Lindner, "OFDM-MFSK as a special case of noncoherent communication based on subspaces," in *Proc. 17th Int. OFDM Workshop (InOWo)*, 2012, pp. 1–5.

[35] G. Yammine, E. Peiker, W. G. Teich, and J. Lindner, "Improved performance of coded OFDM-MFSK using combined alphabets and extended mapping," in *Proc. 8th Int. Symp. Turbo Codes Iterative Inf. Process. (ISTC)*, Aug. 2014, pp. 17–21.

[36] M. Wetz, W. G. Teich, and J. Lindner, "OFDM-MFSK with differentially encoded phases for robust transmission over fast fading channels," in *Proc. 11th Int. OFDM-Workshop*, 2006, pp. 1–5.

[37] H. S. Hussein, A. S. Mubarak, O. A. Omer, U. S. Mohamed, and M. Salah, "Sparse index OFDM modulation for IoT communications," *IEEE Access*, vol. 8, pp. 170044–170056, 2020.

[38] M. Salah, O. A. Omer, and U. S. Mohammed, "Spectral efficiency enhancement based on sparsely indexed modulation for green radio communication," *IEEE Access*, vol. 7, pp. 31913–31925, 2019.

[39] M. Shimaponda-Nawa, O. Kolade, W. Ding, D. N. K. Jayakody, and L. Cheng, "Soft-decision decoding of permutation-based optical codes for a multiple access system," *IEEE Commun. Lett.*, vol. 25, no. 9, pp. 2824–2828, Sep. 2021.

[40] A. Rajesh and R. Nakkeeran, "Performance analysis of integrated system under impulse noise and multipath channel using turbo coded OFDM," in *Proc. 16th Int. Conf. Adv. Comput. Commun.*, Dec. 2008, pp. 254–259.

[41] F. Barrami, Y. Le Guennec, E. Novakov, J.-M. Duchamp, and P. Busson, "A novel FFT/IFFT size efficient technique to generate real time optical OFDM signals compatible with IM/DD systems," in *Proc. Eur. Microw. Conf.*, Oct. 2013, pp. 1247–1250.

[42] H. Elgala, R. Mesleh, and H. Haas, "An LED model for intensity-modulated optical communication systems," *IEEE Photon. Technol. Lett.*, vol. 22, no. 11, pp. 835–837, Jun. 1, 2010.

[43] A. T. Hussein and J. M. H. Elmirghani, "10 Gbps mobile visible light communication system employing angle diversity, imaging receivers, and relay nodes," *J. Opt. Commun. Netw.*, vol. 7, no. 8, pp. 718–735, Aug. 2015.

[44] J. M. Kahn and J. R. Barry, "Wireless infrared communications," *Proc. IEEE*, vol. 85, no. 2, pp. 265–298, Feb. 1997.

[45] J. G. Proakis and M. Salehi, *Digital Communications*, vol. 4. New York, NY, USA: McGraw-Hill, 2001.

[46] A. J. Han Vinck and H. C. Ferreira, "Permutation trellis codes," in *Proc. IEEE Int. Symp. Inf. Theory*, Nov. 2001, p. 279.

[47] O. Kolade, M. Shimaponda-Nawa, D. J. J. Versfeld, and L. Cheng, "Optimization algorithms for improving the performance of permutation trellis codes," *Phys. Commun.*, vol. 44, Feb. 2021, Art. no. 101237.

[48] H. W. Kuhn, "The Hungarian method for the assignment problem," *Nav. Res. logistics Quart.*, vol. 2, nos. 1–2, pp. 83–97, 1955.

[49] L. Liu and D. A. Shell, "Assessing optimal assignment under uncertainty: An interval-based algorithm," *Int. J. Robot. Res.*, vol. 30, no. 7, pp. 936–953, Jun. 2011.

[50] I. J. Cox, M. L. Miller, R. Danchick, and G. E. Newnam, "A comparison of two algorithms for determining ranked assignments with application to multitarget tracking and motion correspondence," *IEEE Trans. Aerosp. Electron. Syst.*, vol. 33, no. 1, pp. 295–301, Jan. 1997.

[51] J. Armstrong and B. Schmidt, "Comparison of asymmetrically clipped optical OFDM and DC-biased optical OFDM in AWGN," *IEEE Commun. Lett.*, vol. 12, no. 5, pp. 343–345, May 2008.

MULUNDUMINA SHIMAPONDA-NAWA received the B.Eng. degree in electrical and electronics engineering from The Copperbelt University (CBU), Zambia, in 2008, and the M.Ing. degree *(cum laude)* in electrical and electronics engineering from the University of Johannesburg (UJ), South Africa, in 2015. She is currently pursuing the Ph.D. degree with the University of the Witwatersrand, Johannesburg, South Africa, which is being funded by the Mwalimu Nyerere African Union Scholarship Scheme and SITA Aero. She worked at Airtel Zambia as a Transmission Planning Engineer and a Team Leader, designing and optimizing the Telco's transport network, for over six years. Her research interests include visible light communications (VLC), powerline communications (PLC), and optical fiber communications (OFC).

OLUWAFEMI KOLADE received the Ph.D. degree from the University of the Witwatersrand, Johannesburg, South Africa. He is currently a Postdoctoral Research Assistant at the Department of Meteorology, University of Reading, Reading, U.K. Prior to this, he was a Postdoctoral Associate on smart grid research at the University of the Witwatersrand, Johannesburg. His research interests include implementation of data assimilation algorithms for climate and weather prediction, signal processing, error correction, and machine learning for communication channels.

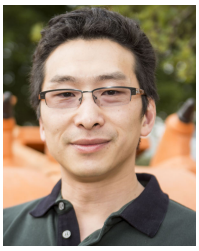

LING CHENG (Senior Member, IEEE) received the B.Eng. degree *(cum laude)* in electronics and information from the Huazhong University of Science and Technology (HUST), in 1995, and the M.Ing. and D.Ing. degrees *(cum laude)* in electrical and electronics from the University of Johannesburg, in 2005 and 2011, respectively. In 2010, he joined the University of the Witwatersrand, Johannesburg, where he was promoted to a Full Professor, in 2019. He has been a visiting professor at five universities and the principal advisor for over 40 full research postgraduate students. He has published more than 100 research papers in journals and conference proceedings. His research interests include telecommunications and artificial intelligence. He was awarded the Chancellor's Medals, in 2005 and 2019, and the National Research Foundation ratings, in 2014 and 2020. The IEEE ISPLC 2015 Best Student Paper Award was made to his Ph.D. student in Austin. He serves as an associate editor for three journals. He is the Vice Chair of the IEEE South African Information Theory Chapter.